The Influence of Unsteady Flow to the Performance of a Horizontal Axis Tidal Turbine

Binoe E. Abuan, and Robert J. Howell

***Abstract*—This paper presents the effect of an idealized cyclic velocity variation to the performance of a Horizontal Axis Tidal Turbine. A steady base case simulated using Reynolds Averaged Numerical Simulation (RANS) was presented to have reference for the unsteady simulations which were conducted for three different tip speed ratios (TSR). Results for the unsteady simulations shows a decrease in performance for all three TSRs (TSR=4, 6 and 8). The cyclic averaged CP for the TSR=6 simulation is 1.94% lower than that of the steady flow case, a decrease of 8% was observed for the TSR=4 case while it is 0.23% difference for the TSR=8 unsteady simulation.**

***Index Terms*—Coefficient of Performance, Horizontal Axis Tidal Turbine, Unsteady Flow Simulations, Unsteady Reynolds Averaged Numerical Simulation**

I. Introduction

One of the renewable energy sources that is gaining attention from both the academic and industrial sector is tidal stream energy; and at the center of researches are the tidal stream energy extraction devices with the Horizontal Axis Tidal Turbine (HATT) as one of the primary focus.

Tidal turbines are designed and analyzed in terms of uniform steady flow whereas the effect of the unsteadiness is not included. This paper will present the performance of a HATT subjected to an idealized unsteady condition induced with the use of a sinusoidal inlet velocity profile with the goal of comparing it with the steady-flow performance and explaining the differences through hydrodynamic analysis. The study is purely numerical and is conducted using Unsteady Reynolds Averaged Numerical Simulations (URANS).

II. Literature Review

A. Steady Flow Simulations and Experiments in Tidal Turbines

Analysis of tidal turbines in steady flow both in physical and numerical simulations has been presented in a number of published literature already. A group in the University of Southampton led by Bahaj et al [1] had conducted a number of experiments both in a cavitation tunnel and a towing tank to be used as validation for numerical modelling with Blade-Element Momentum (BEM) and Computational Fluid Dynamics (CFD) simulations.

In terms of numerical modelling, BEM and Reynolds-averaged Numerical Simulation (RANS) CFD simulations with Large Eddy Simulation (LES) are the ones being used for most studies. The BEM method has been explored and validated by Batten et al [2] and was compared with their experimental results as stated in reference 1. BEM has also been integrated into wind and tidal turbine performance and design software and includes Gerrand Hassan's Bladed and Tidal Bladed has been validated by the Energy Technological Institute (ETI) as well as Batten et al. [2] QBlade, an open source software that is using BEM has been used and validated by the authors for use in tidal turbines [3, 4].

To overcome the limitations of BEM which does not include the real three dimensional flow effects around the blade, CFD (RANS and others) has been used and developed for numerical simulations. Malki et al [5] used a coupled BEM-CFD model to address the limitation of BEM but still have faster simulations than CFD. Investigations of wakes has been carried out by MacLeod et al [6] using a RANS solver with k-ε turbulence closure model and has found that 5 diameter separation is enough for tidal turbines in an array as the velocity/energy is recovered at this distance. RANS has also been used for the investigation of solidity and blade deflection by Morris [7] while the effect of plug flow and high shear flow to tidal turbine was investigated by Mason-Jones et al [8]

B. Unsteady Flow Simulations and Experiments

Tidal turbine performance and hydrodynamics has been studied for steady flow but is still being developed for more realistic and more complicated flow that is happening where tidal turbines are usually installed – unsteady flow.

Although there are available literature in unsteady flow already, most of them are looking at blade (thrust) loading with the main focus being the effect of fatigue loading in unsteady flow to be part of the designing phase for tidal turbine blades. This effect has been shown by Young et al [9] where the maximum von Mises stress in unsteady flow exceeded the design material's yield strength by 65% when compared to steady flow blade loading.

Planar oscillatory experiments conducted by Milne et al [10] shows that there is an increase in blade loads with increased frequency and loads exceeded the steady state blade loads by up to 15% for reduced frequencies between

B. E. Abuan, PhD is an Assistant Professor of the Department of Mechanical Engineering, University of the Philippines Diliman (e-mail: beabuan@up.edu.ph)

R. J. Howell, PhD is a Senior Lecturer of the Department of Mechanical Engineering, University of Sheffield (e-mail: r.howell@sheffield.ac.uk)

ISBN: 978-988-14048-9-3
ISSN: 2078-0958 (Print); ISSN: 2078-0966 (Online)

0.03 and 0.10 with maximum unsteady amplitude of 25%. A phase lead of the blade loads over velocity was also observed, which is an expected effect from dynamic inflow due to unsteadiness.

Another effect on unsteadiness, dynamic stall has also been observed with phase lag and delayed separation for low tip speed ratios (TSR). Dynamic stall effects include variation of velocity over the turbine rotor which will results to changes in lift and drag which are both dependent to the instantaneous angle of attack. These changes results to blade loads not following the steady flow regime and is following a hysteresis curve. This has also been observed by Milne [11] where a 25% increase in blade loading was presented while exhibiting a large degree of hysteresis.

Luznik et al [12] conducted an experiment in a three-bladed HATT with and without waves to look at the effects of waves in performance. Results suggests that the effect of waves is insignificant, for the conditions used, as the values of CP with waves shows similar results with steady data. In terms of flow unsteadiness, one of the very few published papers that looked at performance is the real flow analysis done by Leroux et al [13] using measurements from the Grand Passage, Nova Scotia with results showing very small difference between steady and unsteady flow with only a 0.83% disparity. This is for an unsteady profile with a mean velocity of 2.05 m/s and a maximum amplitude of 10%. Even though the averaged performance was presented, there is no instantaneous analysis present in the paper and the hydrodynamics is also not presented as it is not the focus of the study.

It is true that the device reliability and design is the most important part when it comes to devices like tidal turbines but improving the performance based on the environment and the flow setting where the turbine is installed is also a crucial step in the development of the technology. This is the rationale behind this study to fill the gap in the literature in presenting the effect of flow unsteadiness to turbine performance by presenting instantaneous response and hydrodynamics.

III. The Sheffield HATT CFD Model

A new tidal turbine designed at the University of Sheffield with the blade configuration described in Table 1 has been used for this study. The Sheffield HATT was designed with the aid of QBlade with the goal of having a relatively high coefficient of performance (CP) over a wide range of TSRs which is preferred for a fluctuating inflow velocity. Detailed design specifications and the validation for Qblade has been done by the authors in previous papers. [4].

The CFD model of the Sheffield HATT that has been used for this study was created using ANSYS ICEM-CFD. A detailed mesh independence and boundary size study has been conducted to determine the most suitable mesh for the simulations, see Abuan [4]. The resulting mesh is an unstructured tetrahedral mesh with 300 cells around the foil ar the 75% span of the blade with 15 layers of prism cells generated from the blade surface as shown in Figure 1a. The computational domain and boundary conditions is presented in Figure 1b while the rotational domain was shown in Figure 1c. It should be noted that part of the limitations of this paper is the absence of the free surface as the model was intended to be used for an experimental validation in a cavitation or towing tank. The hub of the rotor was also not included with reference to Kang et al study [14] where it was shown that the inclusion of the hub and the support structure for the turbine has minimal effects for the turbine performance.

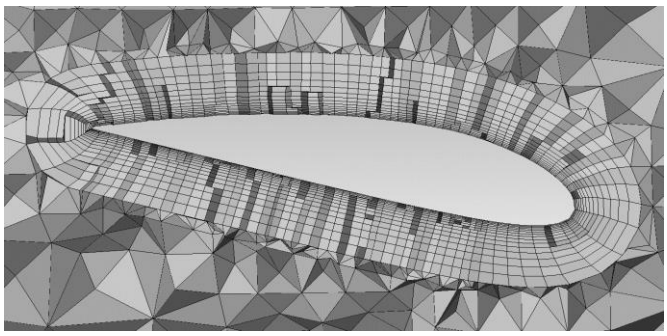

(a)

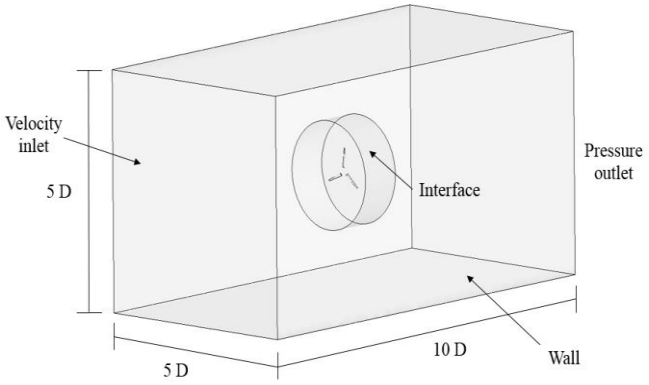

(b)

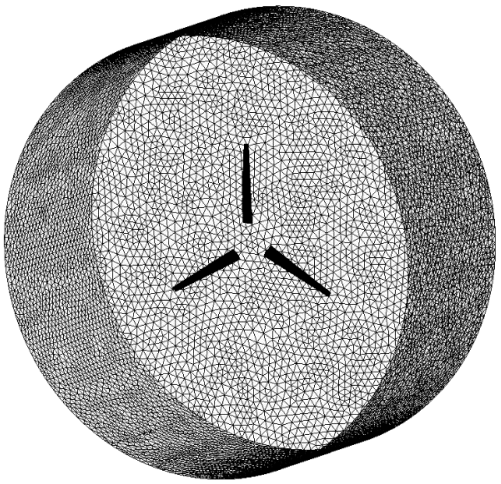

(c)

Fig. 1. Sheffield HATT mesh images; cut plane to show prism layer boundary mesh (a), whole computational domain showing boundary conditions (b), and the rotational domain (c).

ISBN: 978-988-14048-9-3
ISSN: 2078-0958 (Print); ISSN: 2078-0966 (Online)

TABLE I
SHEFFIELD HATT GEOMETRY SPECIFICATIONS

Radial Postion (m)	Chord Length (m)	Twist (°)	Conversion from Gaussian and CGS EMU to SI [a]
0.4	0.25	20	NACA 4424
0.6	0.2312	14.5	NACA 4420
0.8	0.2126	11.1	NACA 4418
1.0	0.1938	8.9	NACA 4417
1.2	0.175	7.4	NACA 4416
1.4	0.1562	6.5	NACA 4415
1.6	0.1376	5.9	NACA 4414
1.8	0.1188	5.4	NACA 4413
2.0	0.1	5	NACA 4412

IV. STEADY FLOW SIMULATIONS

Steady flow simulations were conducted using ANSYS FLUENT's RANS method using k-ω SST turbulence model with resulting y+ values between 30 and 100 which is in the log layer. A water velocity of 2 m/s which is within the range of optimum velocity as quoted from Carbon Trust [15] was used. This corresponds to a Reynolds number of 1,350,000 at the 75% span of the blade. 2nd-order transient implicit formulation was chosen to assure convergence with more iteration per time-step. 2nd order upwind discretization was used since the mesh was made of tetrahedrals not aligned to the direction of the flow. Residual values are allowed to reach 5×10^{-5} for before convergence declaration.

The resulting power curve for the steady flow simulation together with the BEM predicted results from QBlade is presented in Figure 2. It can be seen that the CFD results is lower when compared to the BEM results as a result of three dimensional effects not captured in the QBlade simulations.

.

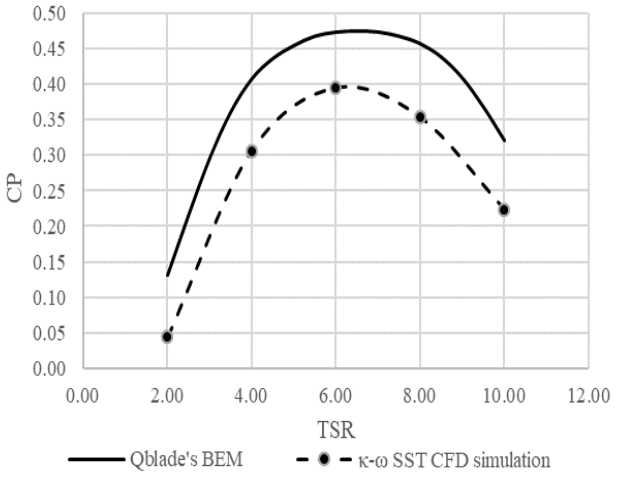

Fig. 2. Power curve comparison between CFD and BEM results for the Sheffield HATT

A steep decrease in the CP was observed as the TSR became lower and this is due to the high angles of attack (AoA) generated in this area. Although high angles of attack means higher lift generated, it could also mean higher drag due to separated flows as shown in the streamline plots for the 25% and 75% span of the blade for TSR=2 in Figure 3. Stall has been observed which will result to two outcomes, a decrease in lift accompanied by an increase in drag resulting to a drastic decrease in CP in Figure 2.

A maximum CP of 39.46% was observed at TSR =6 where the turbine has an optimum performance of lift and drag where the streamlines will be following the shape of the airfoil and although the angle of attack is lower, the lift to drag ratio at this point is the highest thus resulting to the high CP. This will be the reference case for the unsteady flow simulation at the optimum TSR. As the TSR increases, the AoA generated will continue to decrease and the lift to drag ratio will be lower due to smaller. There will also the possibility of having negative lift due to negative angle attack as can be seen in Figure 4 where there is an overlap in the coefficient of pressure (Cp) plot for the 75% blade span signifying the reversal of the angle of attack.

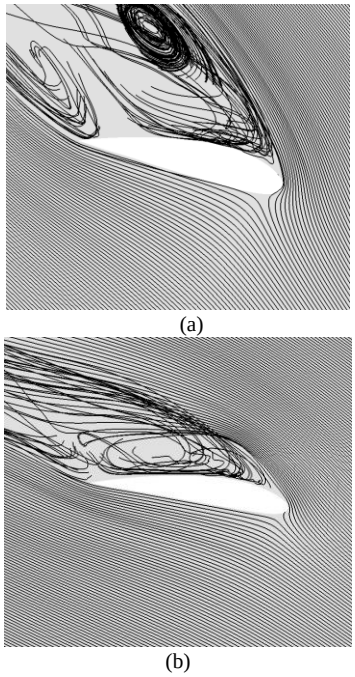

Fig. 3. Streamlines at 25% (a) and 75% (b) spam of the blade at TSR=2 of the Sheffield HATT steady flow simulation

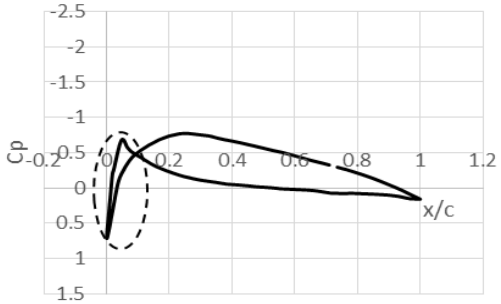

Fig. 4. Coefficient of Pressure plot for TSR=10 at the 75% blade span

V. UNSTEADY FLOW SIMULATIONS

A. Optimum Performance

The peak performance of the steady flow simulation has been used as the basis of the unsteady case, since a turbine would generally be operated at the location of the maximum performance; this case it is at TSR=6 with a CP of 39.46%. The unsteady inflow was induced in the simulation with the use of a User Defined Function (UDF) which uses the equation $u(t) = 1.940061 + 0.49 \sin(2\pi t)$, where t is the flow time. This idealised flow variation has an amplitude that is

ISBN: 978-988-14048-9-3
ISSN: 2078-0958 (Print); ISSN: 2078-0966 (Online)

25% of the mean velocity with a flow frequency of 1 Hz. It is also important to note that this equation was also set to have a cyclic-averaged water power equal to that of the steady flow at 2 m/s. This is to assure that the CP for the two cases can be compared to the same available power from the water.

The reduced frequency (k) defined for this paper is the same as that of Leishman in his works about helicopter rotors and wind turbines [16] which is $k=\pi fc/\omega R$ where f is the frequency of the flow, c is the chord length, ω is the rotational speed and R is the radius of the rotor blade from where you are measuring. It was stated by Leishman that a flow can be assumed to be quasi-steady even if it has variation in the flow if k is between 0 and 0.05. The reduced frequency for this idealised unsteady case at 75% span of the blade is 0.051 which is just outside the quasu-steadiness range.

The simulations were conducted using the same conditions as the steady state simulation but this time, the unsteady inflow was used. Figure 5 shows the resulting instantaneous CP curve for the unsteady simulation and it can be easily seen that it is not following the steady power curve and has formed a hysteresis curve. The hysteresis curve was labelled so that the flow of discussion will be easier and to connect it with other plots that will be provided in the latter part of the paper. It can be seen that the region formed by points b-c-d-e shows instantaneous CP values compared to the steady power curve while the region f-g-h-a las lower CP value. It can be seen that in the right hand part of the hysteresis curve, a steep decrease can be observed. This is due to the low AoA at this region coupled with the sensitivity of the chosen aerofoil for low AoA where as a very steep variation in the lift to drag ration has been observed for the NACA 44xx series, which means for a small change in AoA there is a big change in the instantaneous performance which is dependent in the instantaneous lift to drag ratio.

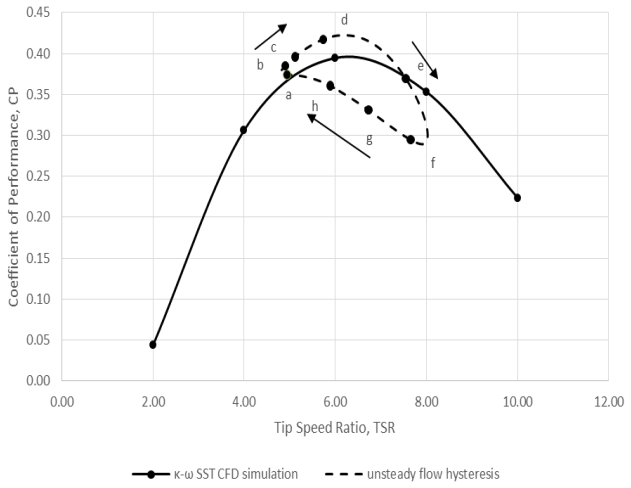

Fig. 5. Unsteady flow hysteresis curve for the TSR=6 unsteady flow simulation over the steady-state power curve.

The instantaneous power extracted by the turbine has been plotted together with the available water power and the unsteady flow velocity as can be seen in Figure 6. The interaction of the two power curves results to the instantaneous CP in Figure 7 plotted with the instantaneous TSR. The cycle-averaged CP, which is defined to be the ratio of the averaged power extracted over the cyclic-power available, for this simulation is 37.5% which is 1.94% lower than its steady flow counterpart. This clearly states that there is a decrease in the power extracted since the power available for both the steady and unsteady cases has the same value. In Figure 6, it can be seen that there is a lag for the instantaneous power extracted with respect to the instantaneous power available, amounting to 2.8% of the normalized flow time, τ, which is defined to the time over the period of one cycle. This lag results to a delay in the increase of the instantaneous CP as can be seen in the left hand side of the plot in Figure 7 specifically between points a and b. In Figure 7, the region highlighted by oval 1 showed a steep increase in CP. At this point, region the extracted power curve that has started to decrease was paired with the power available that has been dropped already again because of the lag observed, this results to an increase in the instantaneous CP which reached a maximum of 42.2%.

A steep decrease in CP, highlighted by oval 2, was observed in Figure 7. At τ=0.528, the power extracted curve has returned to its original value and will start to decrease even further while the power available has already been decreasing at the start of the τ=0.5 mark. Since the denominator of the ratio for the CP has value that has been decreasing earlier than the extracted power, a decrease in value was observed which reaches a value of 28.9% at τ=0.79.

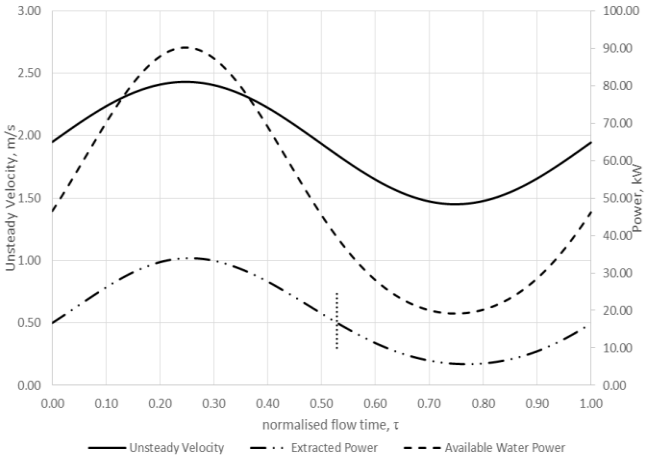

Fig. 6. Instantaneous extracted power and available water power by the turbine with the unsteady velocity profile.

ISBN: 978-988-14048-9-3
ISSN: 2078-0958 (Print); ISSN: 2078-0966 (Online)

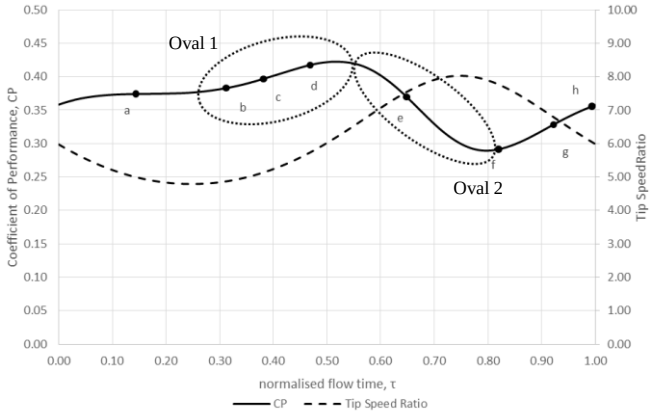

Fig. 7. Instantaneous CP curve for the unsteady velocity over the normalized flow time

B. *Unsteady Flow Simulations at Off-peak Performance*

Two other unsteady flow simulations has been conducted at different TSR (TSR=4 and TSR=8) to further understand the unsteady response of the HATT. For the unsteady TSR=4 simulation, the UDF equation has been altered to $u(t) = 1.9402 + 0.49 \sin(2\pi t)$ with a rotational velocity of 3.8804 rad/s while the equation used for the unsteady TSR=8 simulation is $u(t) = 1.94 + 0.49 \sin(2\pi t)$ for a rotational velocity of 7.76 rad/s. These equations were formulated taking into account the resulting cyclic power available which is still equal to the steady flow power available at 2 m/s. Though the cyclic power available was maintained, the reduced frequency for these two simulations will change. For TSR=4, the value of k at the 75% blade span is 0.068 which is outside the quasi-steady range as per Leishman definition. However, for the TSR=8, the reduced frequency value is only at 0.034, which can be considered as quasi-steady. The changes can be argued to have been reflected in the cyclic-averaged CP which is found out to be 22.6% for the unsteady TSR=4 simulation and 35.1% for the TSR=8 unsteady simulations.

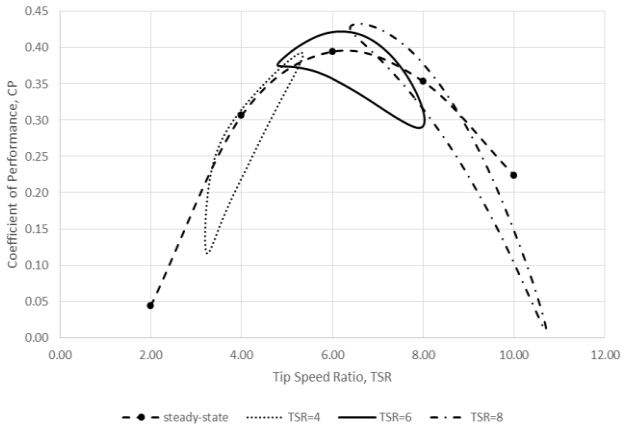

Fig. 8. Complete hysteresis curves for the three unsteady simulations (TSR=4, 6 and 8)

Figure 8 shows the instantaneous CP for the three unsteady cases presented in this paper. It was shown that all of the three cases shows disparity with the steady flow curve and results to hysteresis curves. The hysteresis curve for the TSR=4 simulation shows very steep drop in the instantaneous CP especially for the lowest instantaneous TSR values. Iso-surfaces of vorticity was visualized using the λ_2 criterion plot for the TSR=4 case as it is expected to have a more drastic separation. The formation of vortices at point b in Figure 9 corresponds to the sudden drop in the instantaneous CP in the hysteresis curve as form frag increases due to separation. At point c, it can be seen that the vortex has developed but is still in top of the suction side of the blade, instead of having lower CP, the instantaneous CP at this instance increases because of the increased low pressure developing in the suction side which allowed to lift to go even higher. This effect coupled with the vortices dissipating and the flow reattaching showed further increase in the CP as can be seen in point d of Figure 9. Still, the effect of the increased form drag dominates most of the TSR=4 hysteresis curve which results to a cyclic averaged CP of 22.6% which is 8% lower than the steady state CP at 30.6%.

For the TSR=8 case, we can see a thin but long hysteresis curve and although the flow for this case can be assumed to be quasi-steady, a small difference to the CP value has been recorded as the cyclic averaged CP computed to be 35.1% is still lower than its steady flow counterpart with a difference of 0.23%. The long hysteresis curve can still be attributed to the sensitivity of the aerofoils used for changes at small AoA. One interesting observation about this curve however is that the part of the curve neat TSR=6 is higher than that of the optimum case unsteady simulation which makes up for the very small values of instantaneous CP at high TSR.

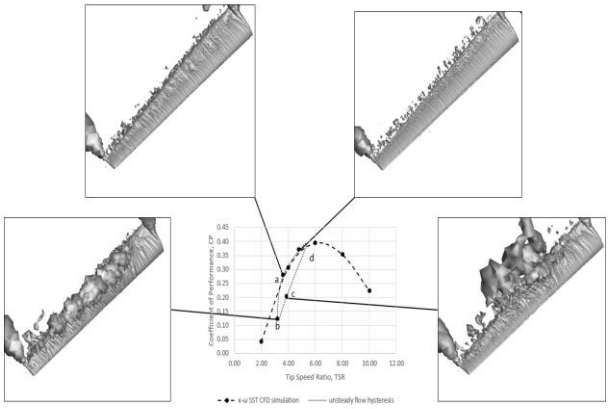

Fig. 9. λ_2 criterion plots for the unsteady TSR=4 simulation

VI. Conclusions

The results of the unsteady flow simulations for the Sheffield HATT shows that the performance of the said turbine under unsteady flow conditions is lower than their steady flow counterparts. At the optimum TSR (TSR=6), the resulting cyclic averaged CP is 39.4% which is 1.94 % lower than that at steady flow. The same observation was seen for the other two unsteady simulations; at TSR=4, the cyclic averaged CP is 22.6%, 8% lower than the steady case value, for the TSR=8, the difference is small relative to the other two simulations as a cyclic averaged CP of 35.1% was recorded which is just 0.23% lower than steady case values.

The main reason observed for the optimum unsteady case

ISBN: 978-988-14048-9-3
ISSN: 2078-0958 (Print); ISSN: 2078-0966 (Online)

simulation is the presence of a lag between the instantaneous extracted power and the instantaneous water power. This results to the instantaneous CP not following the steady flow power curve and resulting into a hysteresis curve. The same observation is present for the other two simulations, thus resulting to hysteresis curves as well. For the TSR=4 simulations, the presence of vortices was also observed and it was shown that a sitting vortex at the suction side of the blade at low TSR also affects the instantaneous CP curve. Overall, from the data gathered using this study, it can be seen that unsteadiness of the flow induced by cyclic velocity variation is detrimental to the performance of the Sheffield HATT.

ACKNOWLEDGMENT

The authors would like to acknowledge the DOST-ERDT project for funding the study and the University of Sheffield for the computing resource used for the simulations.

REFERENCES

[1] Bahaj, A., Batten, W., & McCann, J. (2007). Experimental verifications of numerical predictions for the hydrodynamic performance of horizontal axis marine current turbines. Renewable energy, 2479-2490.
[2] Batten, W., Bahaj, A., Molland, A., & Chaplin, J. (2007). Experimentally Validated Numerical Method for the Hydrodynamic Design of Horizontal Axis Tidal Turbines. Ocean Engineering, 1013-1020.
[3] Danao, L., Abuan, B. and Howell, R. (2016) Design Analysis of a Horizontal Axis Tidal Turbine, 2nd Asian Wave and Tidal Conference. Marina Bay Sands, Singapore.
[4] Abuan, B. and Howell, R. (2016). Effect of Idealised Unsteady Flow to the Performance of Horizontal Axis Tidal Turbine, 2nd Asian Wave and Tidal Conference. Marina Bay Sands, Singapore.
[5] Malki, R., Williams, A., Croft, T., & Masters, I. (2013). A coupled blade element momentum - Computational fluid dynamics model for evaluation of tidal stream turbine performance. Applied mathematical Modelling, 3006-3020.
[6] MacLeod, A., Barnes, S., Rados, K., & Bryden, I. (2002). Wake effects in tidal current turbine farms. Proceedings from Inernational Conference of Marine Renewable Energy. Newcastle.
[7] Morris, C. (2015). Influence of Solidity on the Performance, Swirl, Characteristics, Wake Recovery and Blade Deflection of a Horizontal Axis Tidal Turbine. PhD Thesis. Cardiff University.
[8] Mason-Jones, A., O'Dohetry, D., Morris, C., & O'Dohetry, T. (2013). Influence of a velocity profile & support structure on tidal stream turbine performance. Renewable energy, 23-30.
[9] Young, Y., Motley, M., & Young , R. (2010). Three-Dimensional Numerical Modelling of the Transient Fluid-Structural Interaction Response of Tidal Turbines. Journal of Offshore Mechanics and Arctic Engineering.
[10] Milne, I., Day, A., Sharma, R., & Flay , R. (2016). The characterisation of the hydrodynamic loads on tidal turbines due to turbulence. Renewable and Sustainable Energy.
[11] Milne, I., Day, A., Sharma, R., & Flay, R. (2012). Blade loads on tidal turbines in planar oscillatory flow. Ocean Engineering, 163-174.
[12] Luznik, L., Flack, K. A., Lust, E. E., & Taylor, K. (2013). The effect of surface waves on the performance characteristics of a model tidal turbine. Renewable Energy.
[13] Leroux, T., Osbourne, N., McMillan, J., Groulx, D., & Hay, A. (2016). Numerical Modelling of a TIdal Turbine Behaviour under Realistic Unsteady Tidal Flow. 3rd Asian Wave and TIdal Conference. Marina Bay Sands, Singapore
[14] Kang, S., Borazjani, I., Colby, J., & Sotiropoulos, F. (2012). Numerical simulation of 3D flow past a real-life marine hydrokinetic turbine. Advances in Water Resources, 33-43.
[15] Carbon Trust. (2005). United Kingdom Wave and Tidal Energy Study. Variability of UK Marine Resources.
[16] Leishmann, J. G. (2006). Principle of Helicopter Aerodynamics. Cambridge University Press.

ISBN: 978-988-14048-9-3
ISSN: 2078-0958 (Print); ISSN: 2078-0966 (Online)